

**PRACTICAL ASPECTS
OF
SUPERCONDUCTING RF TECHNOLOGY**

Contents:

- I. Introduction**
- II. Superconductivity**
- III. Surface Defects and Impurities**
- IV. Materials**
- V. Application**
- VI. Surface Resistance**
- VII. Normal RF Surface Resistance**
- VIII. BCS RF Surface Resistance**
- IX. Surface Resistance Due to Trapped Flux**
- X. Examples**

Practical Aspects of Superconducting RF Technology

*John Vincent, Tim Antaya, Dick Blue, John Brandon, Jack Ottarson,
Frans Pigeaud, John Yurkon, Al Zeller*

The NSCL is currently surveying accelerator technologies and nuclear physics research requirements to determine future accelerator needs. A committee was formed on 09/23/92 to look into the current Superconducting RF (SCRF) technology and applications. This note describes the practical aspects of current SCRF theory and technology.

I. Introduction

The investigation of this subject began with a visit to Argonne which specializes in Niobium RF structures. This visit supplied the initial exposure to mechanical formation, chemical treatments, electronic systems, and the operation of Niobium based SRF systems. A committee was formed following this visit to further investigate SRF. An outline of pertinent topics requiring further investigation, based on the knowledge acquired from the visit to Argonne, was supplied to the committee to help steer the investigation.

The committee surveyed the current technology and physics associated with SRF to determine if it was applicable to future NSCL accelerator applications. Papers from leading scientific journals and conferences on the subject were gathered and these materials were compiled into several binders to be used as a reference. Additionally, the committee contacted 8 sites in the US which use and/or develop SRF (3 Lead and 5 Niobium based facilities), and visited 3 of these sites (2 Niobium and 1 Lead based). Reports from these site visits and contacts are also enclosed in the reference binders.

The knowledge acquired from these studies is suitable for evaluating the viability of an SRF project in most circumstances. Should such a system be needed for a future application, the documented experience of many laboratories indicates that a new project could be readily completed if the design does not push the limits of currently operating technology. The SRF portion of an accelerator project should easily fit within the typical 4 - 6 year R&D and construction schedule of a heavy ion accelerator.

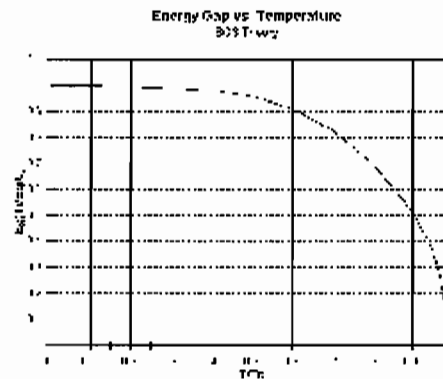
II. Superconductivity

A basic qualitative understanding of the BCS theory of the superconducting state of materials is helpful during the design and development of SRF systems. Some of the commonly used terms are reviewed here.

From a thermodynamic point of view, the transition from the normal state to the superconducting state is a second-order phase transition. A second order phase transition occurs when there is an abrupt change in the specific heat of a material with no corresponding change in the latent heat.

The superconducting state of a metal can be described by loosely bound electron-pairs which are referred to as "Cooper Pairs". The electrons making up a Cooper pair are separated by a distance known

as the "coherence length" denoted by ξ . These paired electrons interact with each other constructively through quantized lattice vibrations known as phonons. The coupled pair of electrons is treated as a boson while the individual electrons are treated as fermions with opposing spin. The electron interaction orders the electrons in k-space with respect to the Fermi sea of electrons. This interaction leads to an energy gap which is equal to two times a pair binding energy " Δ " and varies from 0 at $T = T_c$ to its maximum value of approximately $E_g \approx 3.52kT_c$ at $T/T_c \approx 0.25$. Figure 1 displays the normalized relationship between E_g and T_c from BCS theory. (It is interesting to note that although energy gaps are normally due to electron-lattice interactions, the superconducting state energy gap is due to the electron-lattice-electron interactions.) The energy gap exists between the energy state occupied by the electron-pairs and the energy states which are occupied by normal electrons.

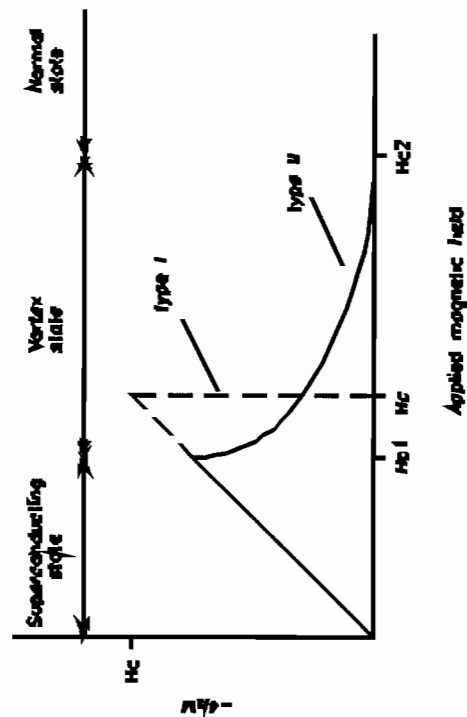


1: Normalized BCS Energy Gap vs. Temperature

At zero frequency, the electron pairs short circuit any normal electrons. At higher frequencies, the inertia of the superconducting pairs increasingly prevents them from totally screening the electric field which allows normal electrons to thermodynamically absorb energy. This last point leads to the BCS surface resistance which is a significant effect in SRF structures at high frequency. It is interesting to note that the distance between a pair of electrons is several hundred angstroms, while the spacing of atoms in the metal lattice is on the order of only a few angstroms.

Two fundamental types of superconducting materials exist which are distinguished from each other by their response to an applied field. For both types of superconductors, the magnetization will increase linearly until it reaches a field value denoted by " H_c or H_{c1} " referred to as the "Critical Field". At the critical field, a "Type I" superconductor can no longer expel the magnetic flux (B) and the magnetization drops to practically zero; whereas, in a "Type II" superconductor the magnetization begins to drop at a gradual rate. At a higher field labeled " H_{c2} ", the Type II superconductor is no longer in the superconducting state. The region in a type II superconductor between H_{c1} and H_{c2} is referred to as the "vortex state" because quantized flux tubes with non-superconducting centers are now penetrating the material. Figure 2 displays the basic relationship between applied field and magnetization for the two types of superconductors.

The fundamental difference between dc applications and rf applications of superconductivity is inherent in the wave behavior of rf fields and losses due to the BCS resistance. In static superconducting magnets, a static magnetic field is created by a dc current imposed at a source point which then follows the path of least resistance to the sink point. Clearly, in a static superconducting magnet, the current will flow around imperfections. A rf current is imposed by a rf magnetic wave on the surface(s) which are guiding it. The major implication of the dc versus rf behavior of the imposed current is that steady state dc currents will flow through the path of least resistance (hence around imperfections), whereas an rf current flows where the rf magnetic field puts it (hence over imperfections). The differences described between dc and rf operating conditions causes the requirements for acceptable operating modes and material processing to be



2: Magnetization vs. Applied Field

substantially different for rf and dc applications. For example, although DC magnetic superconductors may be operated in the 'vortex' state without increased losses, RF surfaces experience large losses in this state.

III. Surface Defects and Impurities

Surface defects have a detrimental effect on the performance of an rf cavity. These defects can create losses from increased surface resistance, or can lead to the creation of emission sites. Thus, advances in reliably obtaining higher microscopic field levels can be linked to the creation of better defect free surfaces. In special cases, dopants can be added to the superconductor to produce beneficial results.

The surface resistance has many well understood sources such as trapped static magnetic flux, surface imperfections, the BCS resistance, and a frequency independent residual element which is not well understood. The low frequency losses are largely dominated by surface imperfections and trapped magnetic flux while the BCS resistance becomes increasingly important as the operating frequency is increased. Defects in the surface can create localized 'normal' regions which can absorb RF power. If the heat generated at the defect is not carried away, the temperature of the surrounding area will rise above the superconducting critical temperature. This results in a normal region which grows outward, and eventually results in a quench.

Lattice impurities decrease the mean free path which causes the coherence length to decrease. As the mean free path is reduced by adding impurities, the BCS resistance first decreases - minimizing when the mean free path is approximately equal to the pure material coherence length - and then increases. For example, a Lead-Tin alloy (2% Tin) has been found to both reduce the BCS resistance and to significantly reduce the oxidation rate.

The RRR (Residual Resistance Ratio) of the material is often used to describe the purity of bulk superconducting materials. This parameter is defined as the ratio between the resistivity at room temperature and the resistivity at 4.2K in the normal conducting state. As the RRR of Niobium approaches 1000, the thermal impedance approaches that of copper. Currently a RRR of a few hundred is commonly available for accelerator applications.

IV. Materials

Niobium and Lead-Tin alloy (2% Tin) are the two materials commonly used in accelerator rf systems. Although Niobium has the greatest future promise for attaining high microscopic fields, the microscopic field levels which are currently and reliably reproduced in practice (about 10 MV/m) are similar for both Lead-Tin and Niobium based systems. However, the lower BCS resistance of Niobium at high frequencies makes it the material of choice over 500 MHz. For both materials, the surface preparation and treatments are a critical manufacturing step, though it should be emphasized that an acceptable defect free surface, suitable for obtaining the current level of reliably operating fields, is obtainable with a modest effort. For a given accelerating gradient, SRF structures should be designed to (1) minimize the microscopic surface fields, (2) minimize the stored electric energy, (3) minimize the thermal impedance to the cryogenic bath, and (4) maximize the mechanical stability. In general, three effects tend to limit the maximum attainable fields: field emission, electron resonant effects such as classic multipactoring, and power limiting due to surface resistance.

Lead-Tin is the simplest and least costly material to apply and is currently better suited than Niobium to larger and more complex cavities. Lead-Tin is normally used as a 2% Tin Lead-Tin based alloy electrically plated onto a chemically polished copper substrate. The Tin is added to reduce the BCS resistance and significantly slow the oxidation of the lead surface as described earlier. Additionally, the tin alloy does not demand chemical post processing of its surface, as required with pure lead. Since the lead is plated onto a copper substrate, it is easy to obtain a very low thermal impedance to the liquid helium source. Due to the excellent thermal characteristics of Lead-Tin based systems, rf fields are typically "limited" by the available rf power and cryogenic capacity assuming no electron effects. A rough description of the surface preparation is, in a

controlled environment (1) create a smooth copper substrate, (2) chemically polish the copper substrate and rinse with high purity water, (3) plate with lead-tin and follow with another high purity water rinse. As a rule, current carrying joints should be avoided, however they may be electron beam welded.

Niobium has a more rugged surface and is currently best suited to structures constructed of pipes (typically interstitial or coaxial structures) or those made of simple small mechanical surfaces (typically parabolic or spherical cavities). Niobium surfaces are typically formed from bulk material, however surfaces constructed of explosively bonded niobium on copper sheet are used at Argonne, and sputtered Niobium is in use at CERN. Niobium has a poor thermal conductivity which makes it thermally unstable unless the Helium bath is in very close proximity to the rf surface. Cavities with high rf fields are sometimes limited by quenching of the superconductor caused by runaway growth of a 'normal' spot in the surface. Sputtered Nb surfaces, however, approach the thermal stability of Lead-Tin based structures and as the purity of bulk Niobium increases, the thermal conductivity also increases. The surface preparation for sputtered Niobium is similar to the description above for PbSn, and likewise, all current carrying joints between components must be electron beam welded. A more elaborate process (not applicable to sputtered or explosively bonded surfaces) would involve repeated annealing cycles which creates a more defect-free lattice and causes impurities to diffuse, or migrate, to the surface where they can be removed. At Cornell, specifically, a titanium gettering process is used to remove surface impurities from bulk niobium structures.

V. Application

In general, SCRF is applicable in situations where 1) no - or very small - static magnetic field exists or is required in the vicinity of the resonator, 2) each structure may be added or removed as a quasi-sealed mechanical entity, 3) a single frequency, or untunable, rf structure is acceptable, 4) large accelerating fields are needed over small spaces, 5) room temperature power costs are excessive for the parameters required, and 6) CW operation is important. Although most laboratories tend to use the SCRF technique they are familiar with, it is possible to make Lead-Tin versus Niobium decisions based on the material properties described.

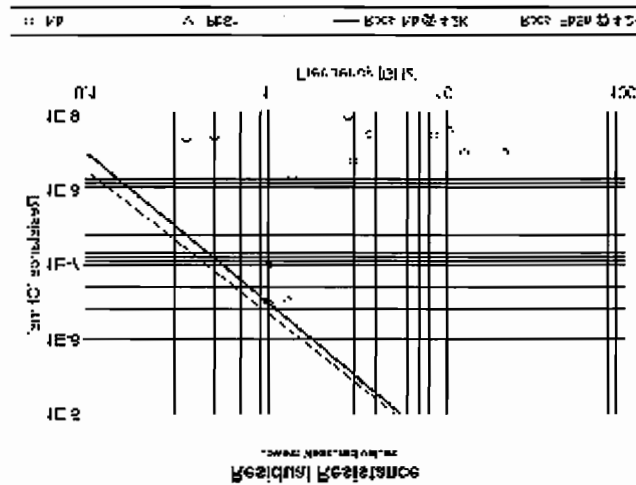
The electronic systems controlling and powering SCRF systems typically consist of broadband power amplifiers controlled by multiple interlaced control loops. The inner most control loop maintains the cavity at resonance with a phase locked loop consisting of a derived phase error representing a frequency error which then drives a DC coupled fm modulation input to the frequency synthesizer. The next surrounding control loop maintains a constant cavity frequency by monitoring the cavity frequency and adjusting a cavity trimmer element. It is preferred that the cavity trimming element not involve mechanical movement except for course initial adjustment. Finally a loop which is nearly independent of the first two attempts to maintain a constant accelerating voltage based on an input reference.

Since there exists a great deal more stored energy in the cavity versus what the limited broadband amplifiers can instantaneously produce, the cavity appears like a massive flywheel to the amplitude control loop. Because of the slow response of the cavity to the amplitude control loop, and to lower the apparent Q of the cavity, the input coupler to the cavity is typically "overcoupled". In the absence of the beam, there will exist an amount of reflected power determined by the amount of overcoupling which is dumped into a load. This tends to lower the apparent Q of the cavity making it more stable to the control loops while also supplying a quasi-reservoir of instantaneously available power to compensate for fluctuating beam conditions which may be intentional or otherwise. This quasi-power-reservoir is created by the coupling and becomes a better match during high load conditions resulting in more power being instantaneously available to the cavity without any control loop intervention. The amplitude control loop can then be matched to the unloaded cavity response while the loaded cavity response is almost completely compensated by the overcoupling condition. It should be noted that whether the power is going into a load or a fluctuating beam, the apparent Q appears nearly constant to the control loops under these conditions.

VI. Surface Resistance

The total surface resistance is a combination of the BCS resistance and other surface resistances. The residual surface resistance is determined from measured values which are largely independent of frequency. Other resistances may be calculated such as resistances due to trapped flux and surface imperfections. Figure 3 shows some measured results for residual resistance in Nb and PbSn with the BCS resistance included for comparison.

$$R_s = R_{BCS} + R_r$$



3: Residual Resistances in PbSn and Nb

VII. Normal RF Surface Resistance

The normal rf surface resistance is

determined by:

$$R_{ns} \sim \frac{1}{\sigma_o \delta_o} \sim \frac{1}{\sqrt{2} \sigma_o \mu_o \omega}$$

where the "skin depth" is defined as:

$$\delta_o \sim \sqrt{\frac{2}{\omega \sigma_o \mu_o}}$$

The previous equations are accurate until a combination of a sufficiently low temperature and high frequency lead to the skin depth becoming approximately equal to the electron mean free path. When the skin depth multiplied by a phenomenological constant equals the electron mean free path the "anomalous skin depth" begins to take effect. In the regime of the anomalous skin depth, only a portion of the total conduction electrons contribute to the material conductivity.

$$\sigma_{\text{eff}} \approx \alpha \left(\frac{\delta_o}{l} \right) \sigma_o \quad \text{for } \alpha \delta_o \leq l$$

where

$$\alpha = \frac{SIMEQ}{3} \approx \frac{1}{2}, \quad l: \text{mean free path}, \quad \sigma_o: \text{normal conductivity}$$

Under the conditions of the anomalous skin effect the effective skin depth and effective surface resistance are then determined.

$$R_{\text{se}} = \left(\frac{\omega \mu_o}{2} \right)^{2/3} \left(\frac{1}{\sigma_o} \right)^{1/3} \alpha^{-1/3} \\ R_{\text{se}} = R_{\text{no}} \left[\frac{1}{\alpha} \left(\frac{l}{\delta_o} \right) \right]^{1/3}$$

$$\delta_{\text{eff}} = \sqrt[3]{2 \frac{\omega \mu_o \delta_{\text{eff}}}{\sigma_o}} = \left(\frac{1}{\alpha} \right)^{1/3} \delta_o^{2/3}$$

The normal conductivity of the material is a function of the mean free path.

$$\sigma_o = \frac{en \mu_o}{m_e} = \frac{e^2 n}{m_e v_f}$$

or

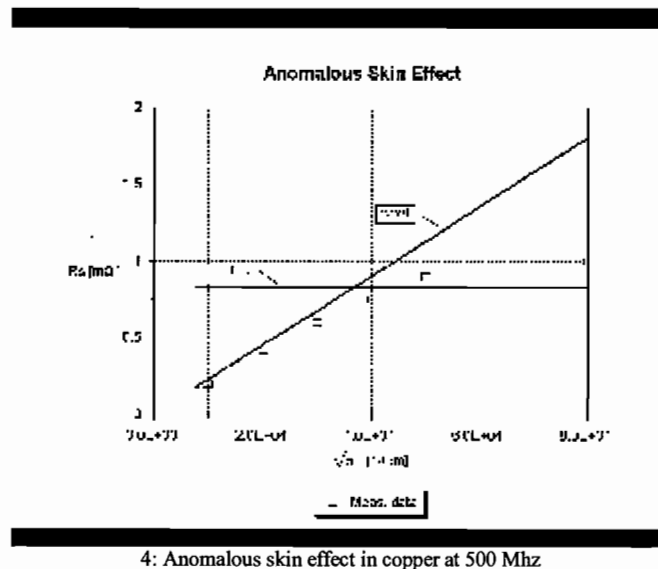
$$l = \frac{v_f m_e}{e^2 n} \quad \sigma_o = A_l \sigma_o$$

$$v_f = \frac{h}{m_e} \left(\frac{3n}{8\pi} \right)^{1/3} \quad \text{and } n = \text{simeq density of atoms}$$

The value of A_1 is best determined by evaluating the ratio of an experimentally measured value of the mean free path at some temperature to the value of the conductivity at the same temperature. If no values of the mean free path are known, then A_1 may be determined purely analytically by the above equations to an acceptable accuracy. Substituting the expression for the mean free path into the expression for R_{sne} shows that the anomalous surface resistance is independent of the material conductivity and varies as $\omega^{2/3}$ which is a characteristic trait of this phenomena. Figure 4 shows measured data for a copper cavity @ 500 Mhz superimposed on the surface resistance curves determined from the equations in this section for both the anomalous and normal regions.

$$R_{sne} \approx \left(\frac{A_1}{\alpha} \right)^{1/3} \left(\frac{\omega \mu_0}{2} \right)^{2/3}$$

The conditional equations described in this section can be used to get a reasonable estimate of the rf surface resistance of a metal in the non-superconducting or "normal" state in both the standard and anomalous regime provided the electrical conductivity as a function of temperature is known.



4: Anomalous skin effect in copper at 500 Mhz

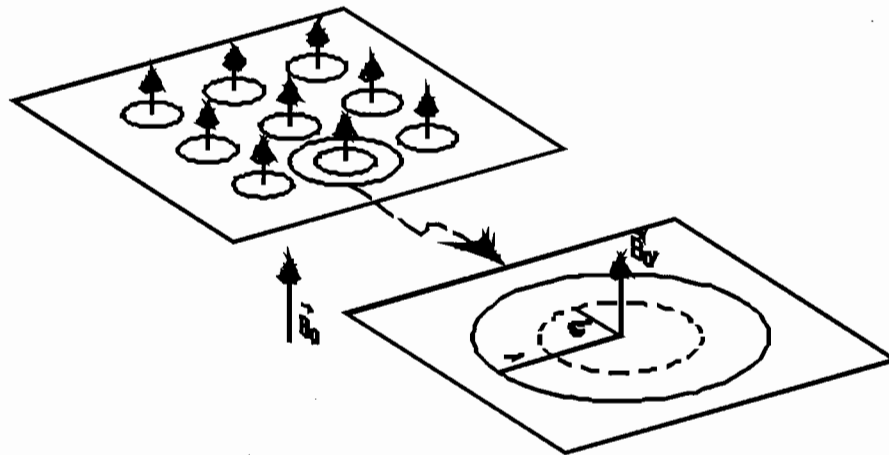
VIII. BCS RF Surface Resistance

The following table contains some useful approximate physical parameters of typical Lead-Tin or Niobium surfaces. Actual unsimplified results of the BCS theory for $0.1 < T < T_c$ and for any E_g require a computer program.

Physical Parameter	2% Lead-Tin	Niobium
T_c : Critical Temperature	7.5 °K	9.25 °K
H_c : Critical Field	803 Gauss	1980 Gauss
2 DELTA SIMEQ $3.52kT_c E_g$: Energy Gap	$4.02kT_c 2.60 \times 10^{-3} \text{ eV}$	$3.90kT_c 3.11 \times 10^{-3} \text{ eV}$
$\{2 \hbar v_F\} \text{ over } \{\hbar E_g\} \zeta_0$: BCS Coherence Length	$8.3 \times 10^{-6} \text{ cm}$	$3.8 \times 10^{-6} \text{ cm}$
$\kappa = \lambda_L \text{ over } \xi_0$: Ginzburg-Landau Parameter	0.45	1.02
$\xi_0 \kappa = \sqrt{m \text{ over } \{e^2 n_s \mu_s\}} \lambda_L$: London Penetration Depth	$3.74 \times 10^{-6} \text{ cm}$	$3.88 \times 10^{-6} \text{ cm}$
R_{BCS} : BCS Surface Resistance $\{A \omega^2 \text{ over } T\} e^{\{-\text{DELTA over } \{kT\}\}}$ $\hbar \omega \leq E_g$ $T \text{ PRECEQ } T_c \text{ over } 2$	$6.85 \times 10^4 f^{1.9} \text{ over } T$ $e^{\{-2.01 T_c \text{ over } T\}} f : \text{Ghz}$ $T : ^\circ\text{K}$ $R : \Omega$	$1 \times 10^5 f^2 \text{ over } T e^{\{-1.95 T_c \text{ over } T\}} f : \text{Ghz}$ $T : ^\circ\text{K}$ $R : \Omega$

IX. Surface Resistance Due to Trapped Flux

In type II materials (such as Niobium) and in thin layers of type I materials (such as lead), static magnetic fields which are imposed perpendicular to the surface may get trapped. The flux would be trapped in quanta of flux (Φ_0) arranged in islands of radius (λ). The material in the center of the island will have



5: The Vortex Effect

the normal conductor value of surface resistance out to a radius equal to the coherence length (ξ) which is shown schematically in figure 5.

DC currents tend to flow around these areas whereas rf currents flow over them as described earlier. This leads to increased conduction losses for the rf case.

The penetration depth is determined from the following:

If $\xi \leq \lambda_L$ then

$$\lambda = \xi$$

otherwise

$$\lambda = \xi \left(\frac{\lambda_L}{\xi} \right)^2$$

The quantum of flux is determined from:

$$\phi_0 = \frac{hc}{2e} \approx 2.07 \times 10^{-7} \text{ Maxwells}$$

The magnetic flux density in each tube is:

The number of quantized flux tubes "n" which would form on a surface area "A" is $B_0' \approx \frac{\phi_0}{\pi \lambda^2} \approx (B_0)^2$ for a type II material)

then:

$$n \approx \frac{B_0 A}{\phi_0}$$

The normal surface area is then:

$$A_n \approx n \pi \lambda^2 \approx \frac{B_0 A}{\phi_0 \pi \lambda^2}$$

If " R_{fs} " is defined to be the overall equivalent surface resistivity due to flux trapping and " R_n " is the surface resistivity of the normal non-superconducting surface then:

$$R_{fs} \approx \frac{R_n \{A_n\}}{A} \approx \frac{R_n \{B_o\}}{\phi_o \pi \xi^2} \approx \frac{R_n (B_o / B_n)}{(\xi^2 / \lambda^2)}$$

The previous analysis and equations are only valid if the static imposed field is both uniform and normal to the entire surface. If this is not the case then the surface resistance becomes a strong function of position and must be retained within the integration for surface losses

$$P_1 \approx \frac{R_n \pi \xi^2}{2 \phi_o} \int_S \{ \vec{B} \cdot \vec{n} \}^2 dS$$

where \vec{n} is a unit vector normal to the surface and pointing into the cavity.

X. Examples

This section uses the techniques described to determine some specific examples which are useful in comparing the conduction losses of resonators which have various combinations of normal and superconducting surfaces. This analysis assumes the resonators are mechanically identical. Under low loss conditions, the field distributions in the resonators will then be identical. With these imposed conditions, the resonant frequency, mode, and stored energy will be kept nearly constant while the surface material is varied. Assuming the surface resistance is not a function of the surface location, the Q may be expressed as:

$$Q = \frac{\omega U}{P_{\text{loss}}} = \frac{\omega \int_V \frac{\epsilon}{2} E^2 dV}{\int_S \frac{R_s}{2} |H_{\text{vec}}|^2 dS}$$

Under the imposed conditions, the two cavities only differ by the conduction losses on the surface so that :

$$\frac{Q_1}{Q_2} = \frac{P_{\text{loss}2}}{P_{\text{loss}1}} = \frac{R_{s2}}{R_{s1}}$$

The following table lists the Q for various materials at two different frequencies normalized to Nb at 500 Mhz at 4.3 °K (Q_0). The table assumes no imposed static magnetic fields.

Material	Q/Q ₀ @ 500 Mhz	Q/Q ₀ @ 1 Ghz
Nb	1.0	0.26
PbSn	0.22	0.19
Cu	1.1 x 10 ⁻⁴	7.7 x 10 ⁻⁵

The following table lists the Q with flux trapping for Nb at two different frequencies and 4 different static field values at 4.3 °K. The table is normalized as above.

Bo (Gauss)	Q/Q ₀ @ 500 Mhz	Q/Q ₀ @ 1 Ghz
0.0	1.0	0.26
0.10	0.20	0.10
1.0	2.5 x 10 ⁻²	1.0 x 10 ⁻²
10.0	2.5 x 10 ⁻³	1.0 x 10 ⁻³

References

1. Tinkam, M.: "Introduction to Superconductivity", Kreiger Publishing Company, Malabar, Florida, 1975.
2. Ibach, H., Luth, H.: "Solid-State Physics", Springer Publishers, New York, 1986
3. Kittel, C.: "Introduction to Solid-State Physics", John Wiley & Sons, Inc., New York, 1986.
4. Turneure, J. P., et-al,: "The Surface Impedance of Superconductors and Normal Conductors: The Mattis - Bardeen Theory", Journal of Superconductivity, Vol 4, No. 5, 1991.
5. Assman, W., et-al,: "Triton Progress Report", Technical University of Munich.
6. Dietl, L., Trinks, U.: "The Surface Resistance of a Superconducting Lead-Tin Alloy", Nuclear Instruments and Methods in Physics Research, A284, 1989, pp. 293-295.
7. Grundey, T., et-al,: "The Superconducting Accelerating Cavities for the Triton", Nuclear Instruments and Methods in Physics Research, A306, 1991, pp. 21-26.
8. Weingarten, W.: "Superconducting Cavities", Proceedings of the CERN Accelerator School, RF Engineering for Particle Accelerators, Exeter College, Oxford, U.K., April, 1991, pp. 381-348.
9. Bardeen, J., Cooper, L. N., Schrieffer, J. R.: "Theory of Superconductivity", Physical Review, Vol. 108, No. 5, 1957, pp. 1175-1204.
10. Editor: Anderson, H. L.: "Physics Vade Mecum", American Institute of Physics, 1981, p. 121.